Electronic Supplementary Material (ESI) for Nanoscale Horizons.
This journal is © The Royal Society of Chemistry 2023

Supporting information

Ultra-sensitive NH_3 gas sensor enabled by ion-in-conjugated polycroconaine/$Ti_3C_2T_x$ core-shell composite

Jin Zhou,[a] *Seyed Hossein Hosseini Shokouh,*[a] *Linfan Cui,*[b] *Topias Järvinen,*[a] *Olli Pitkänen,*[a] *Zhong-Peng Lv**[c] and *Krisztian Kordas**[a]

[a]*Microelectronics Research Unit, Faculty of Information Technology and Electrical Engineering, University of Oulu, P.O. Box 4500, FIN-90014 Oulu, Finland*

[b]*Department of Chemical and Metallurgical Engineering, Aalto University, FIN-00076 Aalto, Finland*

[c]*Department of Applied Physics, Aalto University, FIN-00076 Aalto, Finland*

E-mail: zhongpeng.lyu@aalto.fi; Krisztian.Kordas@oulu.fi

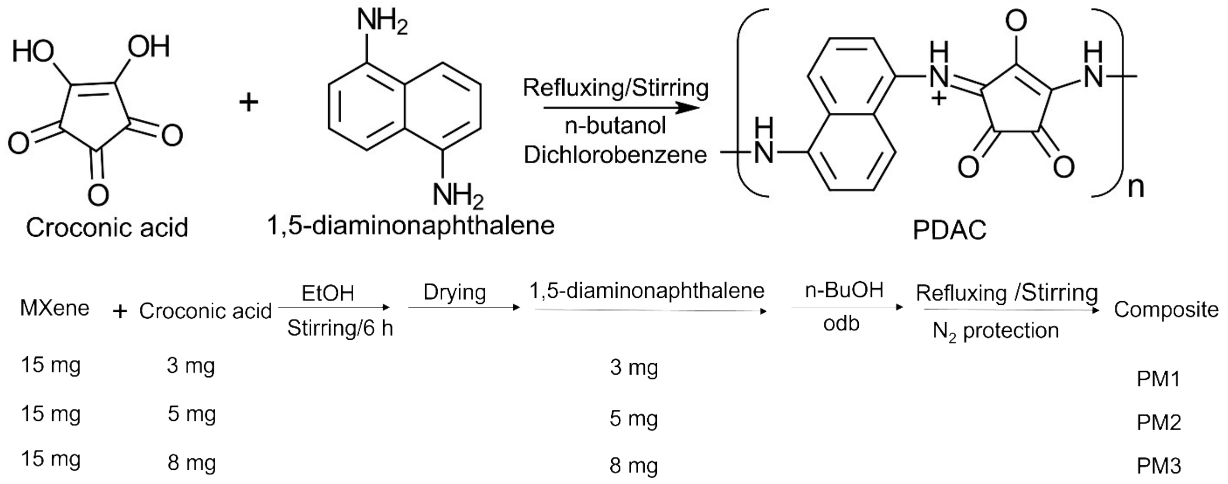

Fig. S1 Synthetic routes to PDAC, and the preparation process of PM1, PM2 and PM3.

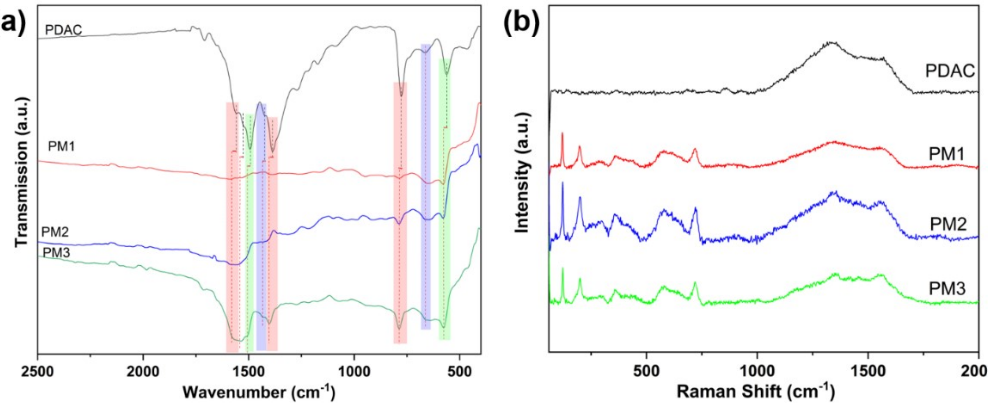

Fig. S2 (a) The FTIR spectra and (b) Raman spectra of the $Ti_3C_2T_x$@PDAC hybrid in different ratios.

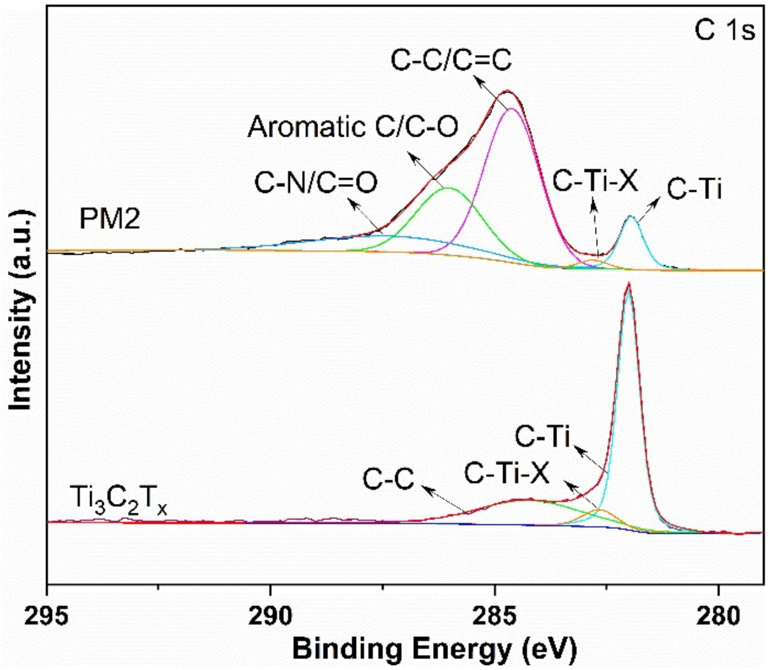

Fig. S3 C 1s XPS spectra of PM2 and pristine $Ti_3C_2T_x$.

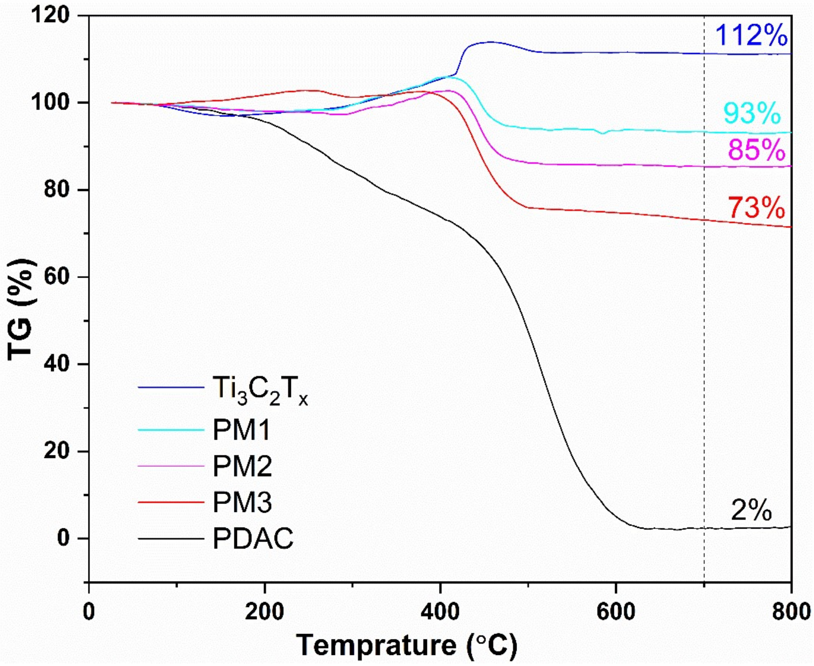

Fig. S4 TGA curve of PDAC, $Ti_3C_2T_x$ and their hybrid in different ratios. As the temperature increases, the mass of Ti_3C_2Tx increases due to the formation of TiO_2, which involves the absorption of oxygen. To calculate the mass ratio of $Ti_3C_2T_x$ and PDAC in the hybrid, we assume that they are completely converted into the final product, and the total mass is only composed of the following components: $x+y=1$, where x and y are the mass ratios of $Ti_3C_2T_x$ and PDAC in the hybrid. The final TG value of sample z can be written as $1.12x+0.02y=z$, by solving the above two equations, we can derivate the value of x and y. For example, in the case of PM2, $z=0.85$, the solution of the equation is $x=0.75$ and $y=0.25$.

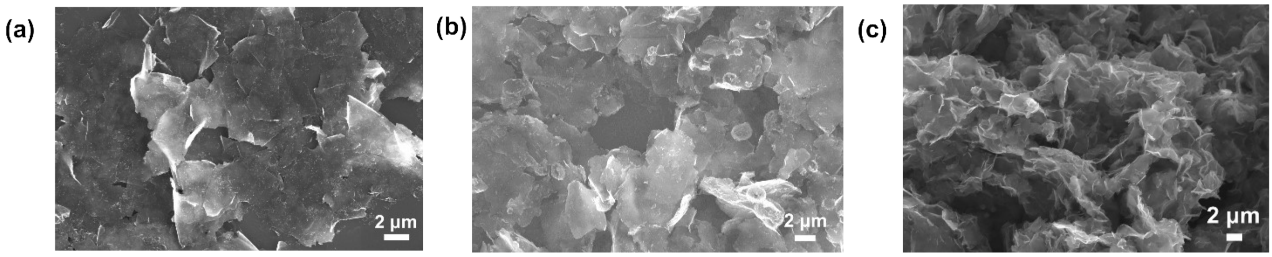

Fig. S5 SEM image of (a) PM1, (b) PM3 and (c) $Ti_3C_2T_x$.

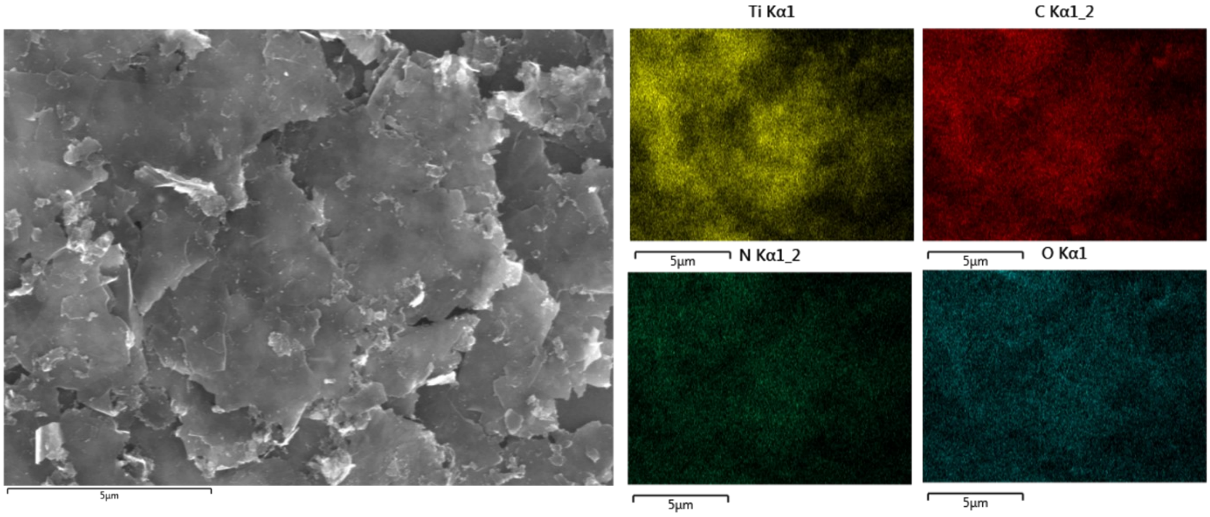

Fig. S6 Elemental mapping of PM2.

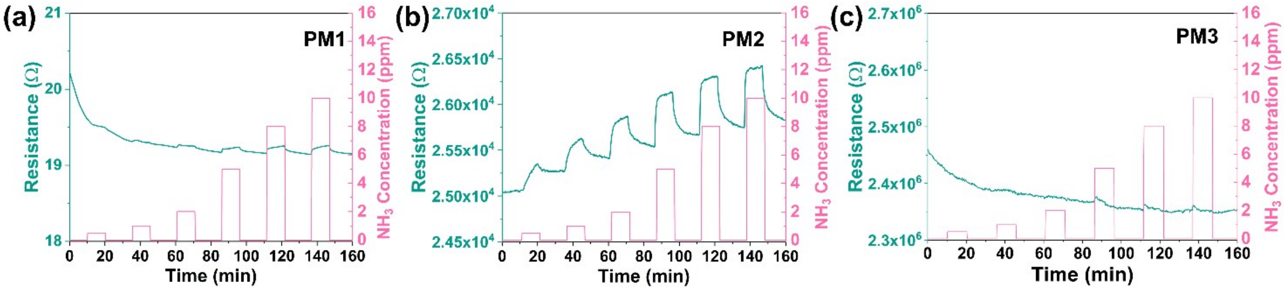

Fig. S7 Real-time sensor resistance of (a) PM1, (b) PM2 and (c) PM3 under 0.5, 1, 2, 5, 8 and 10 ppm NH_3. The time intervals labelled with the red periods indicate the introduction of NH_3 to the test chamber.

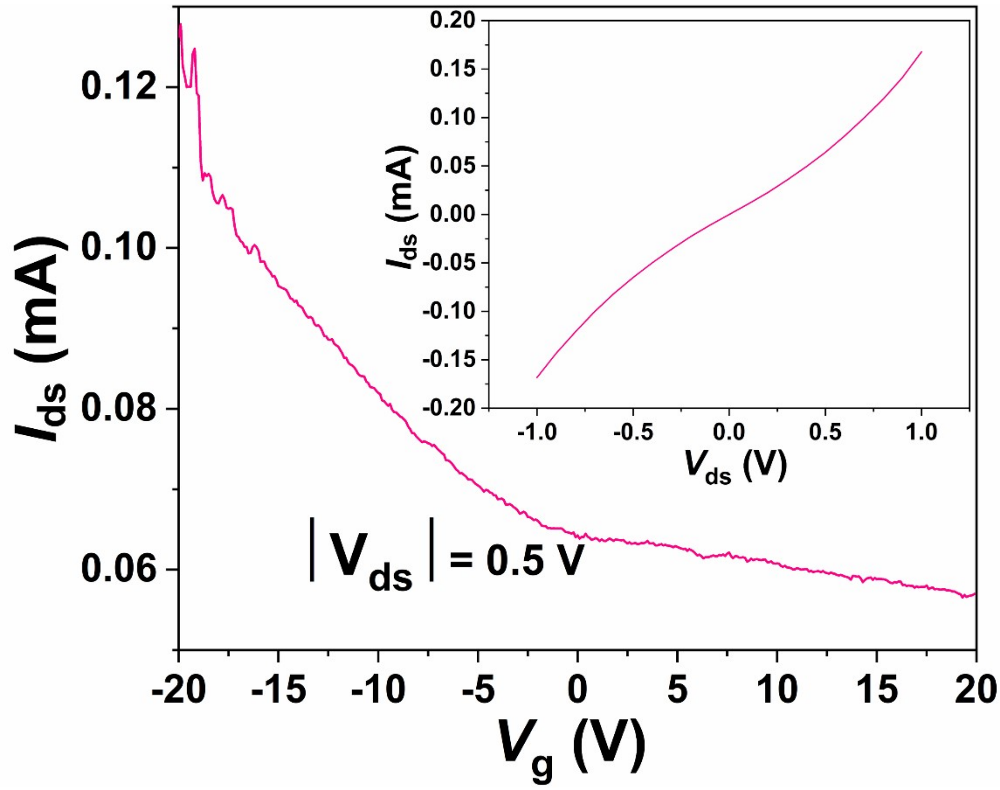

Fig. S8 Transfer and I–V (inset) characteristic curves of composite-based FET-type device.

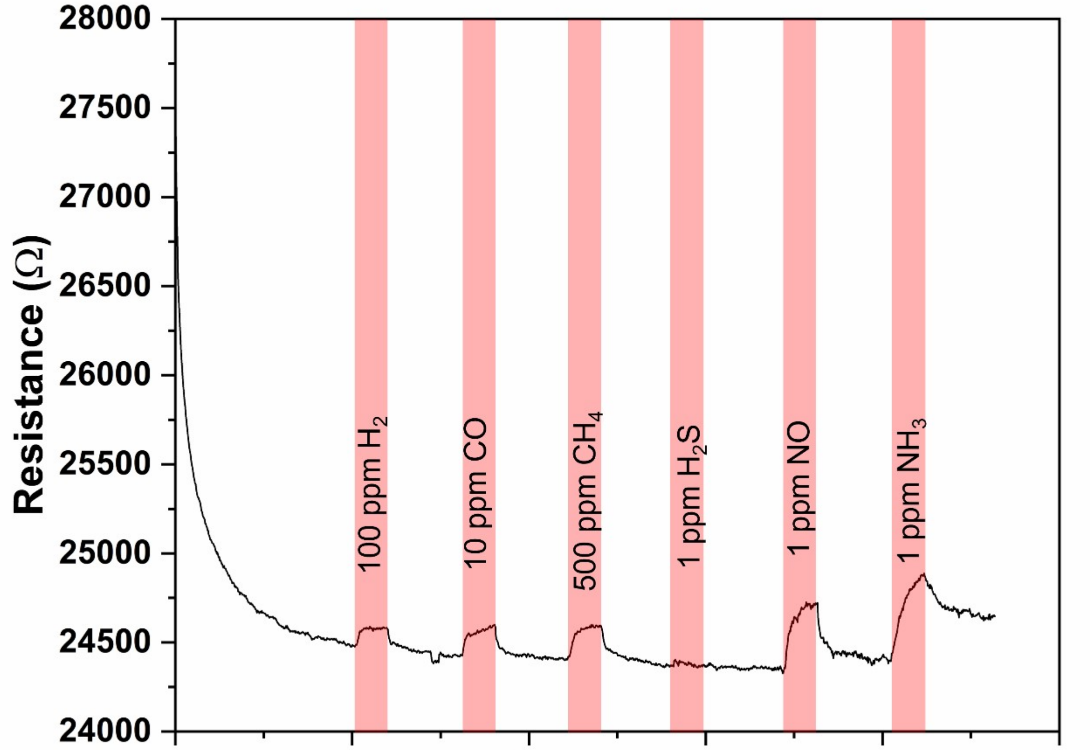

Fig. S9 Real-time sensing resistance of the PM2-based sensor changes with different gases.

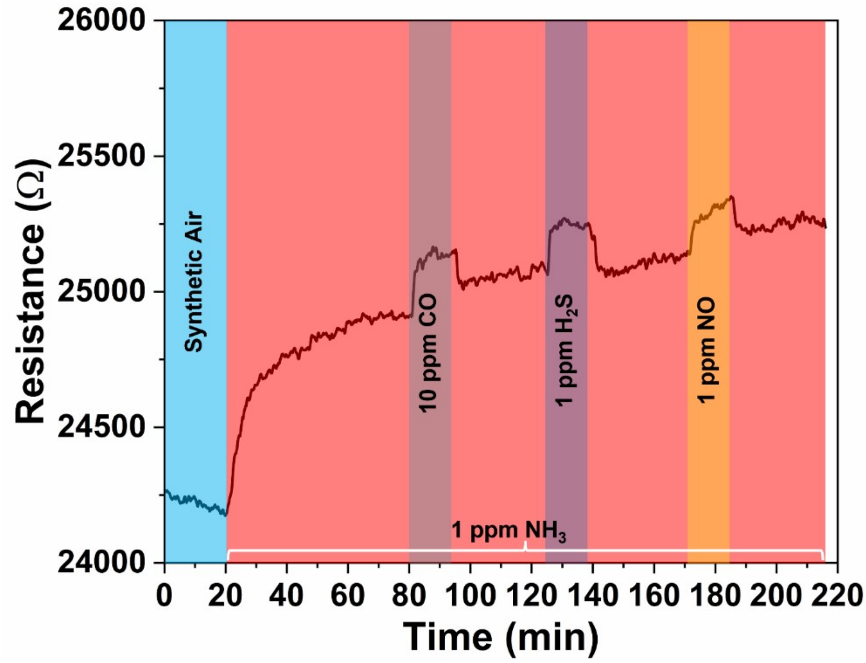

Fig. S10 Sensor resistance variation upon exposure with binary mixtures of analytes (NH_3 and interfering gases such as CO, H_2S, and NO).

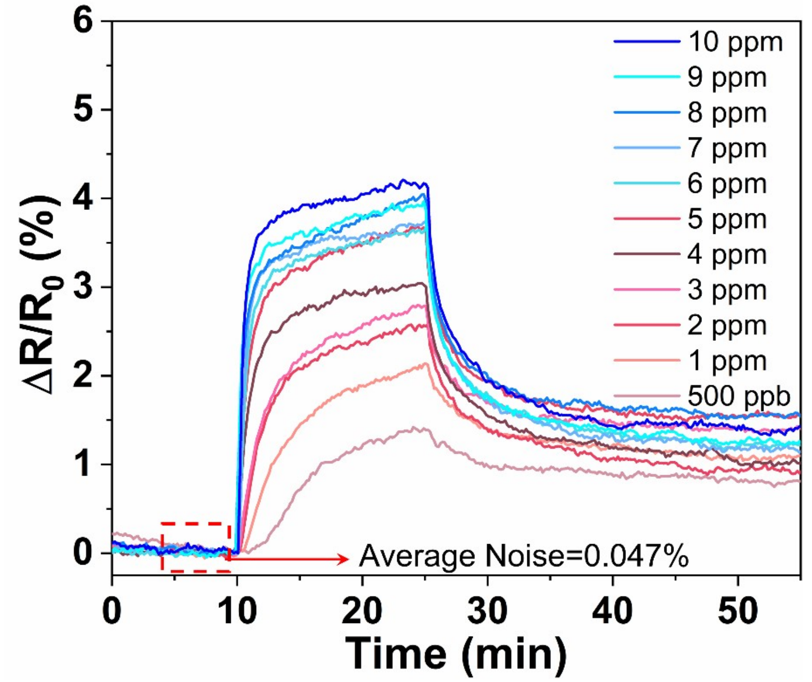

Fig. S11 (a) Noise occurred in the process of sensing measurement. The noise is defined as the standard deviation of the datapoint without the gas analytes exposure. The average noise is the average value of the noise in the above 11 measurements. The LOD is calculated by 3SN/sensitivity, i.e., 0.141%/(2.8%/ppm) ≈ 50 ppb.

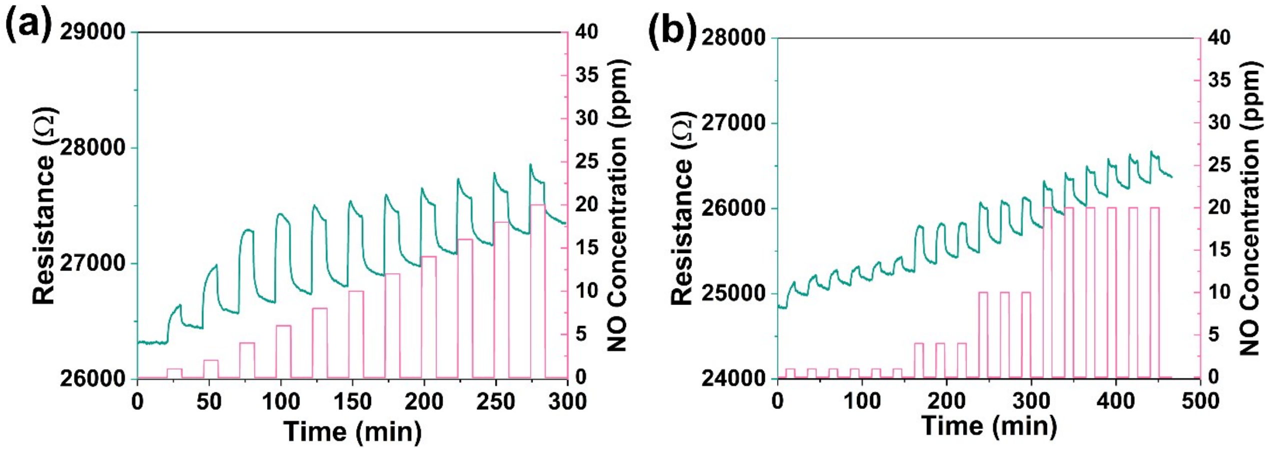

Fig. S12 NO sensing performance. (a) sensor resistance variation under different NO concentrations; (b) repeatability of the sensor at 1, 4, 10 and 20 ppm NO. We further investigated the sensor performance towards NO detection in the range of 1 ppm to 20 ppm. Similar to that measured for NH_3, the response is nonlinear with the concentration and shows good repeatability. It is interesting to note, that the profile of the measured electrical signals gradually changes with the increase of the NO concentration. When introducing the gas pulse of a higher concentration (at above 6 ppm), the resistance firstly increases i.e., the analyte acts as an electron donor for the p-type semiconducting surface, and then, a decay of resistance change can be observed within the same gas pulse. Such a decreased resistance suggests electron withdrawal from the surfaces, presumably due to the oxidation of NO to NO_2 having a pronounced oxidizing character.

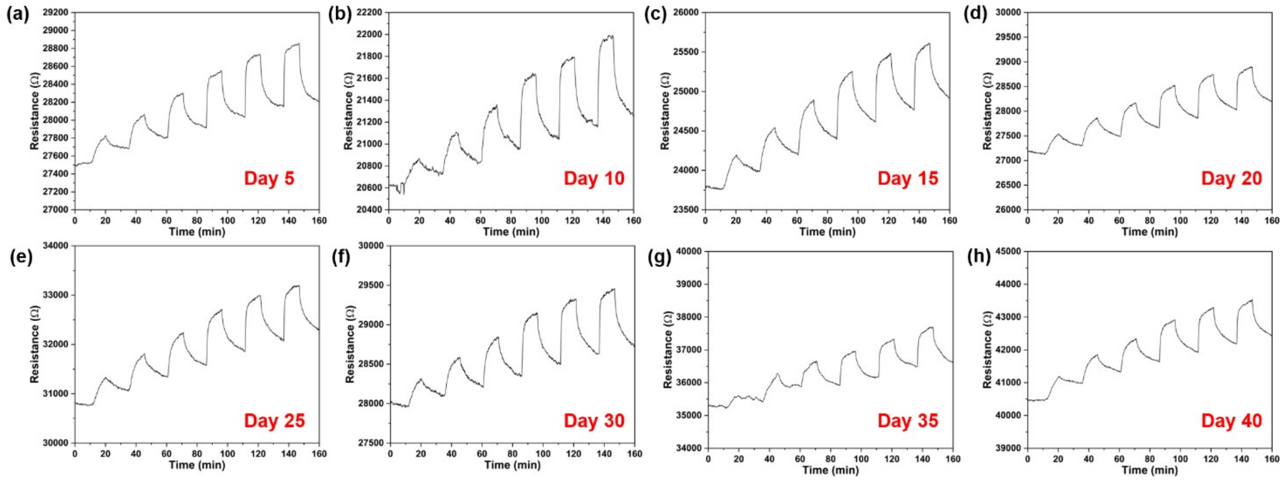

Fig. S13 The real-time sensing resistance changing of PM2-based senor under 0.5, 1, 2, 5, 8 and 10 ppm NH_3 in 40 days.

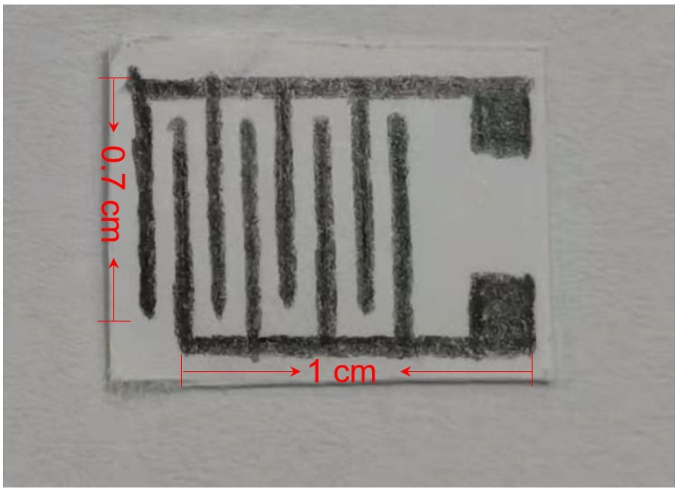

Fig. S14 Photographic image of paper substrate with graphite interdigital electrode.

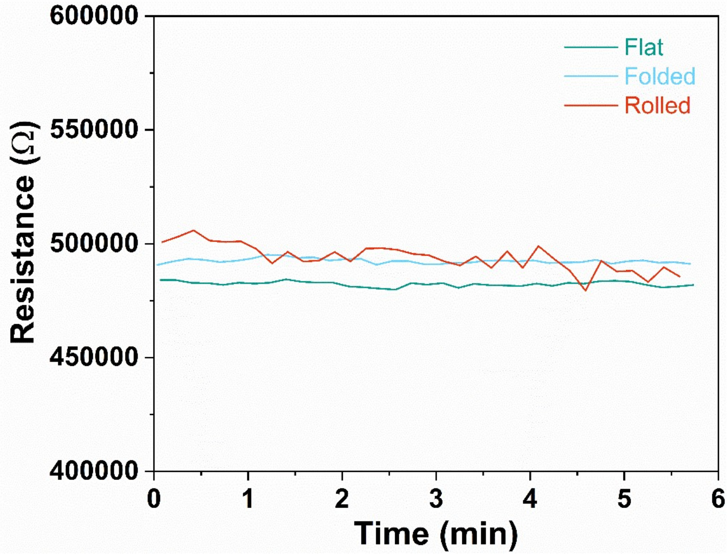

Fig. S15 The base resisitance of the paper-based sensor in different situations without gas flow.

Fig. S16 Spray coated pattern on the print paper made by PM2. (The mask is made by the Al_2O_3, and the concentration of the ink is about 5 mg/mL)

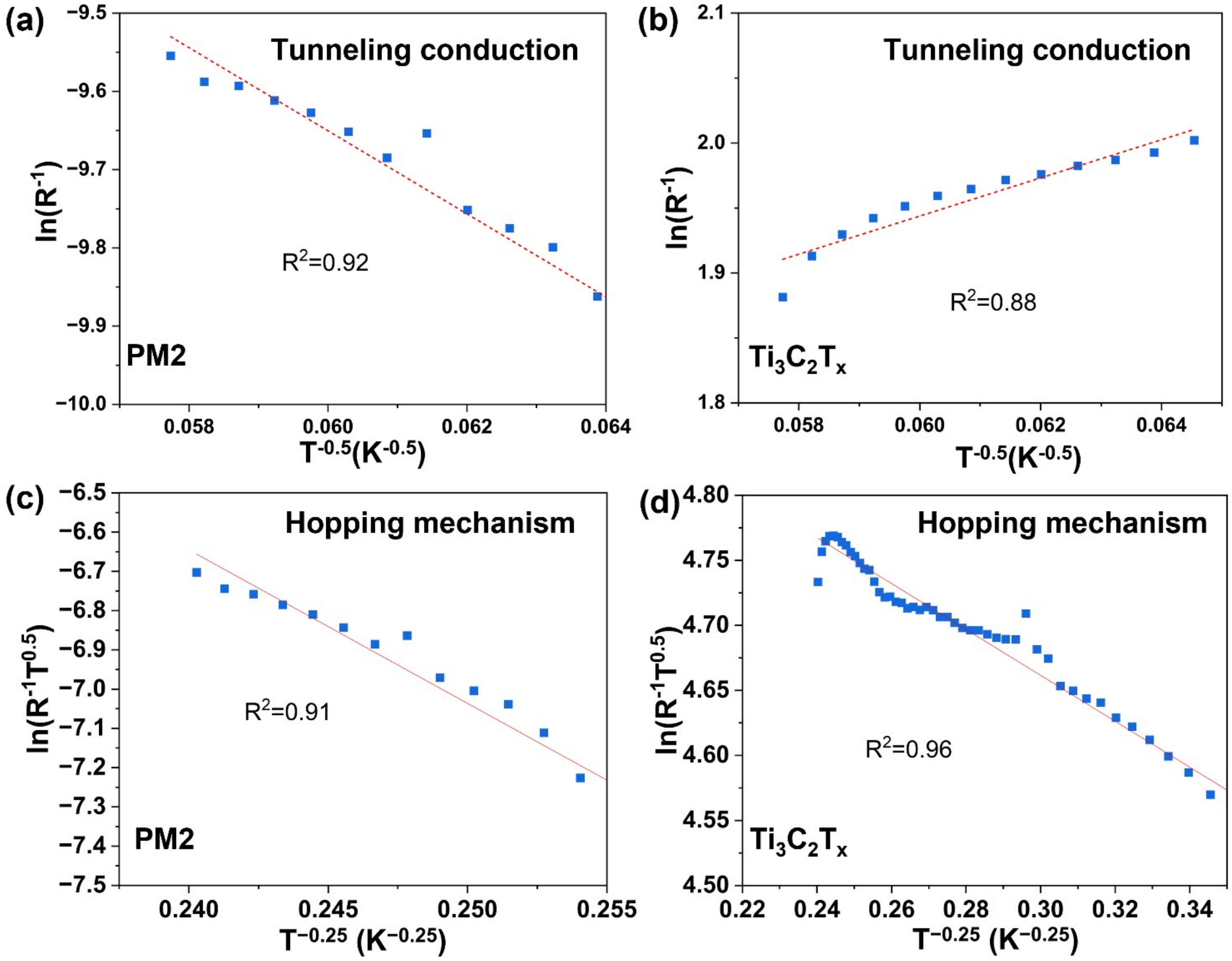

Fig. S17 Linear fitting curve of data shown in Fig. 5. (a, b) Plot of $\ln R^{-1}$ versus $T^{-1/2}$ and (c, d) plot of $\ln(R^{-1}T^{-1/2})$ versus $T^{-1/4}$.

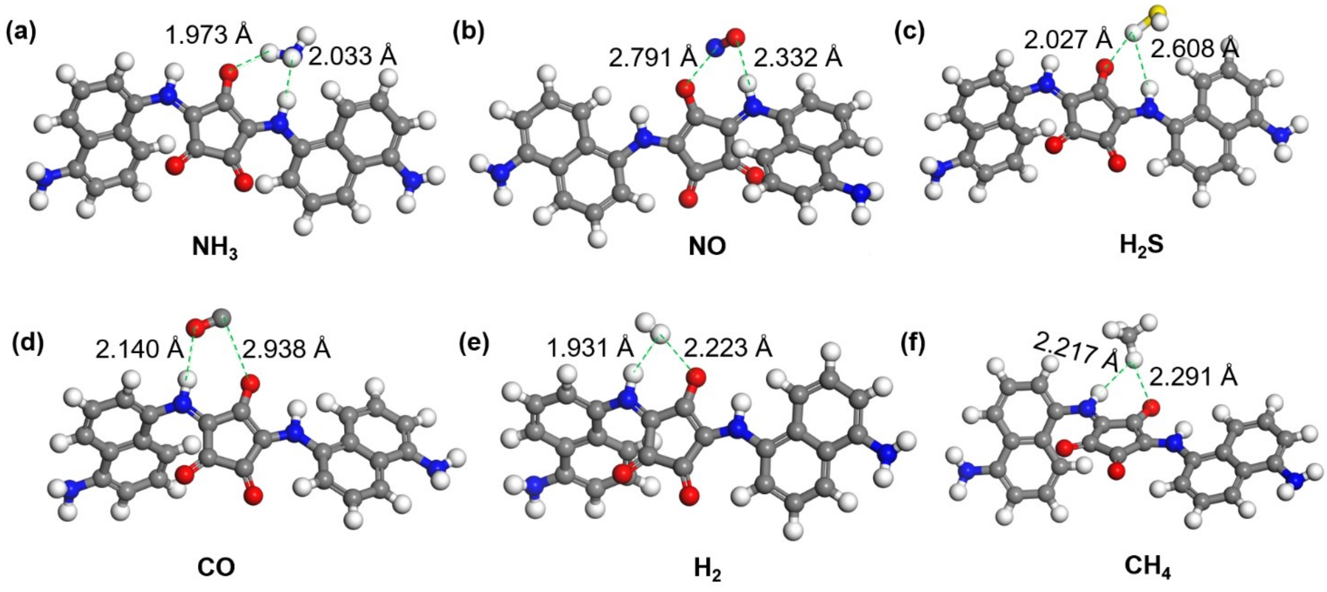

Fig. S18 Simulated adsorption modes of different analytes on the PDAC.

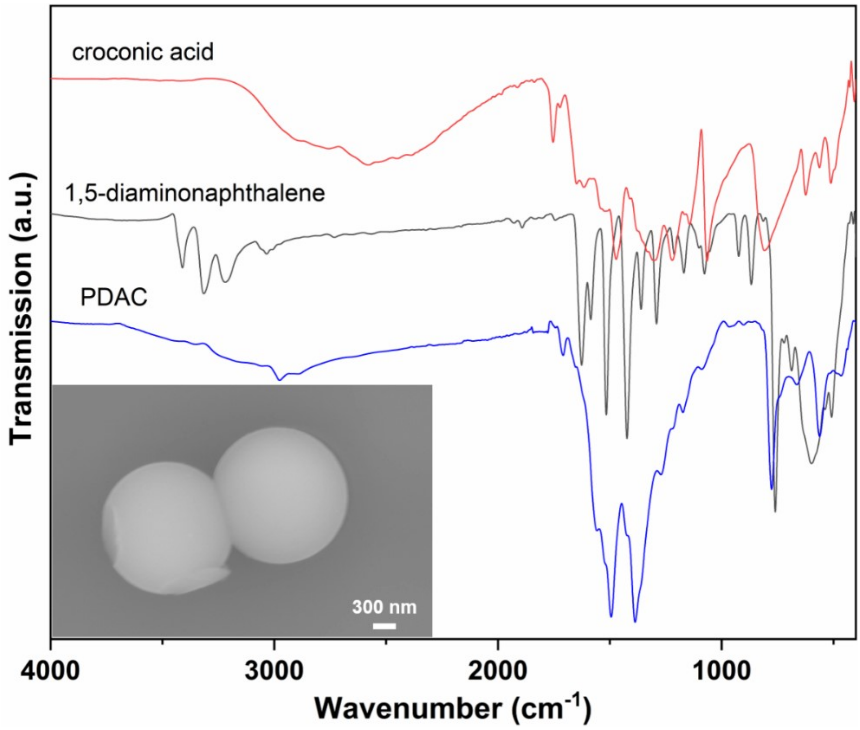

Fig. S19 FTIR spectra of reactants and the PDAC. The peaks over the 3000 cm^{-1} are attributed to the -N^{+}H= group in the PDAC. Inset: SEM image of the PDAC, which shows a sphere-shaped microstructure with a diameter of around1.8 μm.

Table S1. The binding energies and charge transfer of different analytes adsorbed on PDAC.

Analyte	Binding energy (eV)	Charge transfer (e^-)
NH_3	**0.54**	**0.072**
NO	0.11	−0.070
H_2S	0.47	0.042
CO	0.12	0.007
H_2	0.10	0.018
CH_4	0.19	0.0023